Master of Science Thesis

Dynamics of Andean flat slab formation viewed in a mantle reference frame

Gerben Schepers

July 2015

Faculty of Geosciences
Department of Earth Sciences
Utrecht University

Supervisors:
Douwe J.J. van Hinsbergen, Lydian M. Boschman and Wim Spakman

Abstract

The 7000 km long Andean fold-thrust belt formed during ~1400 km absolute westward motion (Doubrovine et al. 2012) of the South American Plate, overriding the subducting Nazca Plate (Russo & Silver 1996; Oncken et al. 2006). The slab of subducted Nazca Plate lithosphere followed this motion and has rolled back. Only in two segments the Nazca Plate is sub-horizontal, over a distance of 200-300 km (Barazangi & Isacks 1976; Cahill & Isacks 1992; , and therefore has a different amount of roll-back in these segments. Flat slabs have pronounced effects on orogenesis (Ramos et al. 2002) and magmatism (Stern 2004) and are widely believed to be caused by the downgoing plate resisting subduction(Gutscher et al. 2000; Pilger 1981). Here we show a kinematic reconstruction of the Andean fold-thrust belt and restore the Andean trench migration in a mantle reference frame (Doubrovine et al. 2012; O'Neill et al. 2005). We demonstrate that since the onset of slab flattening, 11-12 Ma (Jordan et al. 1983; Ramos & Folguera 2009), ~1000 km of Nazca Plate subduction occurred, more than three times as much as the flat slab lengths. All Nazca lithosphere that subducted since the onset of slab flattening has thus bypassed the flat slab and disappeared deep into the mantle. The Andean flat slabs thus result from a resistance against roll-back rather than against subduction. We identify trench-parallel absolute motion of the slab and sub-slab mantle resisting lateral escape below buoyant portions of the subducting plate as potential causes. Our study highlights the importance of stydying the dynamics of subduction systems in an absolute plate motion context.

Thesis

The friction between the continental crust of the overriding South American plate, and the subducting oceanic Nazca plate that caused the Andean fold-thrust belt is thought to be the result from a westward 'absolute' plate motion of the South American plate relative to the mantle, overriding the subducting Nazca Plate (Russo & Silver 1996; Oncken et al, 2006). Seismicity and earthquake hypocenters reveal that along 'Peruvian' and 'Pampean' segments, the Nazca Plate is subducting as flat slabs beneath the South American Plate over 200-300 kilometres in the direction of subduction(Barazangi & Isacks 1976; Gutscher et al. 2000; Cahill & Isacks 1992; Hayes et al. 2012) (Fig.1a). With slab pull assumed as major driver of subduction (Turcotte & Schubert 1982), the dynamic causes of such flat slabs are intriguing. A key step toward assessing the possible causes of their generation is to reconstruct their kinematic evolution.

Inferred geological expressions of flat slab subduction can help to date the slab flattening. Such expressions inferred to reflect enhanced plate coupling include the migration of the volcanic front towards the overriding plate, a lateral expansion of arc magmatism, and a migration of deformation towards the hinterland and retro-foreland basin subsidence (Ramos & Folguera 2009). This way, the onset of the Peruvian flat slab subduction was dated at ~11 Ma, and the Pampean flat slab at ~12 Ma (Jordan et al. 1983; Ramos & Folguera 2009). Other segments of the Andean subduction zone may have experienced episodes of flat slab subduction since ~42 Ma (Ramos & Folguera 2009).

The Andean flat slabs were proposed to result from positive buoyancy of subducting oceanic crust due to enhanced volcanism along e.g. the Nazca and Juan Fernandez Ridges (Pilger 1981; Gutscher et al. 2000; Yáñez et al. 2001) (Fig. 1a). The reconstructed moment of arrival of these ridges at the trench may indeed coincide with the onset of flat slab subduction, but no direct correlation was found between previous episodes of flat slab subduction and so-called bathymetric impactors (Skinner & Clayton 2013). Alternative proposals invoke effects of the upper plate, mantle wedge suction (van Hunen et al. 2004; Manea et al. 2012), or heterogeneities in the continent's thickness (O'Driscoll et al. 2012) instead of positive buoyancy of the subducting plate, but remain generic.

Whereas the dynamic causes of formation of the Andes have long been viewed in a so-called mantle reference frame (Oncken et al. 2006; Russo & Silver 1996), the formation of the Andean flat slabs, which reside in and at the top of the mantle, has not. To portray flat slab subduction in its appropriate, 'absolute' plate motion context, we therefore aim to restore the Andean subduction zone and the flat slabs relative to the mantle.

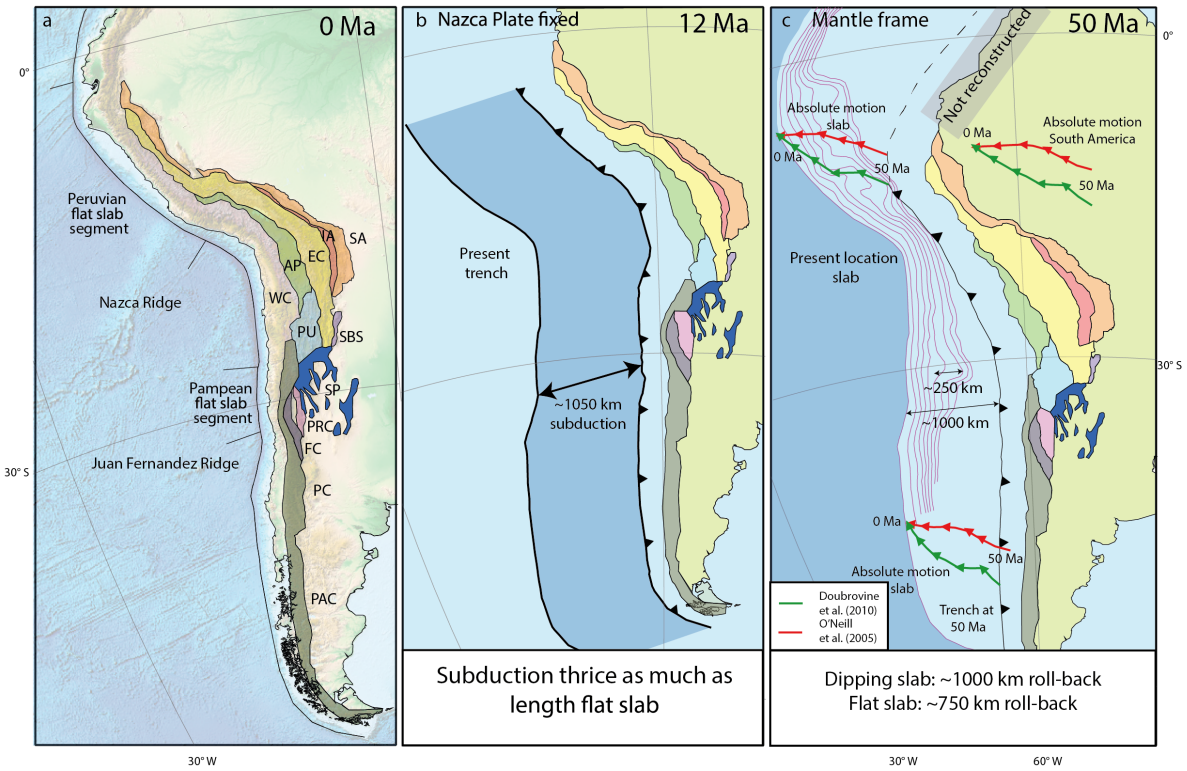

Figure 1. a) Tectonic map (3D Globe projection) of the Andes modified from Kley et al. (1999) and Eichelberger & McQuarrie (2015), showing the boundaries of deforming geomorphologic regions, flat slab segments and ridges as discussed in this paper. Abbreviations are WC, Western Cordillera; AP, Altiplano Plateau; EC, Eastern Cordillera; IA, Interandes; SA, Subandes; PU, Puna Plateau; SBS, Santa Barbara System; PC, Principal Cordillera; FC, Frontal Cordillera; PRC, Precordillera; SP, Sierras Pampeanas; PAC, Patagonian Cordillera.

b) Reconstruction of the Central and Southern Andean fold-and-thrust belt at 12 Ma with a fixed Nazca Plate, colours of the deforming geomorphologic regions are the same as in Figure 2a. The distance between the present trench and the trench at 12 Ma equals the amount of subduction of the Nazca Plate underneath the South American Plate since 12 Ma, shown here in darker blue.

c) Reconstruction of the Central and Southern Andean fold-and-thrust belt at 50 Ma in a hotspot mantle reference frame (O'Neill et al. 2005), colours of the deforming geomorphologic regions are the same as in Figure 2a. The purple lines represent the present depth contour lines of the Nazca Plate from 0-160 km with a 20 km interval (Hayes et al. 2012). The amount of slab roll-back for a dipping slab perpendicular to the present depth contour lines is ~1000-1100 km, for the flat slab segment this is ~250 km less. The lines with arrows represent the motion paths of the trench and South America since 50 Ma to its present position in steps of 5 Myr from respectively Doubrovine et al. (2012) in red and O'Neill et al. (2005) in green.

To this end, we first define our terminology (Fig. 2). Our reconstruction considers the following kinematic vectors: the **O**verriding South American plate (O), the **D**owngoing Nazca Plate (D), the **T**rench (T), the slab **B**end (B) and the upper **M**antle (M). The trench is defined as the intersection between the subduction thrust and the sea floor and the slab bend as the hinge between the (sub-)horizontal and dipping portions of the subducting plate. In cases of flat slab subduction the slab bend is separated from the trench by an extended zone of low-angle subduction (Fig. 2). Kinematic relationships between these vectors are here illustrated in 1D along a velocity line (Cox & Hart 1986) (Fig. 2). The difference between the motion vectors of the overriding and the downgoing plate is then the *plate convergence rate,* defined as *O minus D*; of the trench and the downgoing plate is the *subduction rate (T minus D)*; of the trench and the overriding plate is the *overriding plate contraction or extension rate (T minus O)*; of the slab bend and the trench is the *flat slab formation or destruction rate (T minus B)*; of the trench and

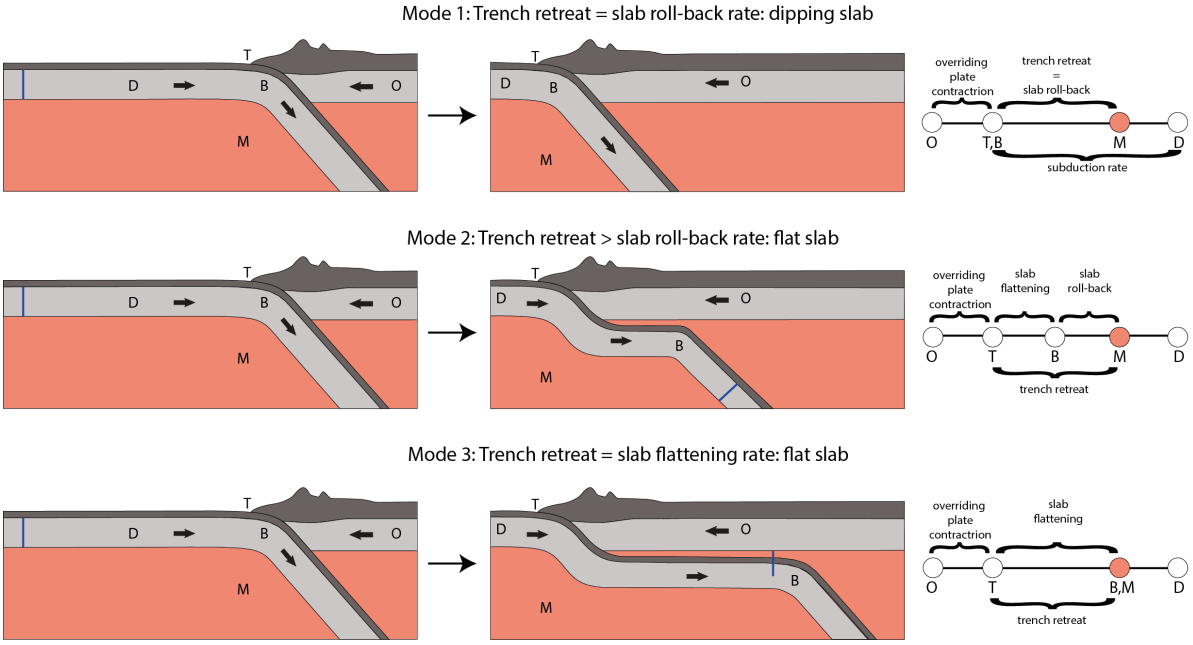

Figure 2. Conceptual model of the onset of slab flattening in a mantle reference frame. Left panel: Plates in a cross-sectional view in stage 1. Centre panel: Plates in a cross-sectional view in stage 2. Right panel: Plates and plate boundaries on a velocity line where point M = mantle is our reference [see e.g. (Cox & Hart 1986)]. Mode 1 represents subduction of a dipping downgoing slab D underneath the overriding plate O. The trench T and slab bend B have the same relative velocity with respect to the mantle, therefore the trench retreat equals the slab roll-back. The higher velocity of the overriding plate O relative to the mantle, compared with that of the trench and slab bend, is accommodated by overriding plate contraction. The blue line on the downgoing plate represents a locally thickened part of the downgoing plate.

Mode 2 represents subduction of a flat slab. The trench T has a higher relative velocity than the slab bend, this results into a higher rate of trench retreat than rate of slab roll-back, i.e., flat slab formation. Note that the blue line passes both the position of the trench and the slab bend.

the mantle is the *trench retreat or advance rate (T minus M)*; and of the slab bend and the mantle is the *slab roll-back or advance rate (B minus M)* (Fig. 2)

Moving hotspot reference frames show that since 50 Ma, the South American plate has moved ~1400 km to the WNW(Doubrovine et al. 2012; O'Neill et al. 2005) (Fig. 1c). If no roll-back or overriding plate shortening would have occurred, flat slabs of this length would have formed (Fig. 2c). The Andean flat slabs are considerably shorter, which is a combined effect of overriding plate shortening, decreasing the amount of trench retreat, and slab roll-back (Fig. 2b). To quantify the latter, we kinematically restored the shortening accommodated in the Andean fold-thrust belt relative to South America. Knowing the age of flat slab formation (Jordan et al. 1983; Ramos & Folguera 2009), the Nazca Plate subduction rate, the current dimensions of the flat slabs (Cahill & Isacks 1992; Hayes et al. 2012), and absolute South American plate motion (Doubrovine et al. 2012; O'Neill et al. 2005) we can then quantify the relationship between the flat slab length (200-300 km(Cahill & Isacks 1992; Hayes et al. 2012) and the amount of subduction since the onset of flat slab formation.

We reconstructed the Andean fold-thrust belt using a total of 50 published balanced cross-sections from 3 degrees S to 56 degrees S, subduction erosion estimates, strike-slip-fault reconstructions, thermochronology data, and paleomagnetic data (see Supporting Information). Because the past positions of the slab bend are poorly constrained, we assumed that at the onset of formation of the Andes around 50 Ma no flat slabs were present. If flat slabs were present 50 Ma the position of the slab bend would be located more eastwards compared with a dipping slab, therefore the estimated amount of roll-back is a minimum. This implies that the amount of roll-back at dipping slab segments equals the amount of trench retreat (Fig. 2a).

Our restoration uses Gplates free plate reconstruction software (Boyden et al. 2011) (Supplementary Information) and reconstructed maximum estimates of Andean shortening, which leads to a minimum amount of trench retreat. The Northern Andes is not reconstructed in detail, as it lies north of the flat slab segments and contains added complexity due to interaction with a third (Caribbean) plate (Boschman et al. 2014; Pindell et al. 1988).Our reconstruction shows maximum shortening estimates of 380 km at the centre of the Bolivian orocline, comparable to previous estimates(Eichelberger & McQuarrie 2015), decreasing to the north and south to 142 and 163 km, respectively. We place this reconstruction in the South America-Antarctica-Nazca plate circuit, and place this in a moving hotspot reference frame (Doubrovine et al. 2012; O'Neill et al. 2005).

With Andean shortening reconstructed and deducted from the amount of WNW-ward absolute plate motion of South America, we can now analyse the evolution of the Andean trench and the formation of flat slabs in a mantle reference frame. A dipping, 'non-flat' slab must have

undergone a net amount of slab roll-back that is equal to trench retreat, whereas a flat slab had a lower net amount of roll-back than trench retreat (Fig. 2).

Approximately 1000 km of Nazca plate has passed the trench since the 12 Ma onset of flat slab subduction (Fig 2b), more than three times the modern width of the flat slabs. Any crust that started subducting ~12 Ma ago must therefore have long passed the slab bend and currently reside much deeper in the mantle: it obviously has not resisted subduction for 12 Myr. If the timing of onset of flat slab subduction is correct, a positive buoyancy of oceanic crust alone cannot have caused slab flattening. We envisage that the causes of flat slab formation should rather be sought in context of the rapid roll-back rate that the Nazca plate must have undergone over its 7000 km width. Roll-back, rather than subduction, was impeded and the amount of slab roll-back in the flat slab segments was lower than the trench retreat.

Roll-back requires that mantle material from below the slab flow to a position above the slab. This occurs through torroidal flow around the edges or through holes, and polloidal flow around its base, if possible (Faccenda & Capitanio 2013). This offers a resistance against roll-back that becomes larger, the farther away from the slab edges (Schellart et al. 2007), which may be explain why the most shortening, and hence the most friction, occurred in the central segment of the Andes (Russo & Silver 1996). The locations of the flat slabs, however, are north and south of the central segment of the slab, and may not be directly explained this way. Furthermore, roll-back induced flow in the upper mantle exerts a viscous drag at the upper-lower mantle boundary that is ~7000 times larger than the total slab buoyancy force (Schellart et al. 2007), which would impede roll-back once the slab reaches the base of the upper mantle. This is not the case in our reconstruction, since the Pampean flat slab segment underwent a minimum amount of roll-back of ~750 km compared to ~1000 km to its north and south (Fig. 2c). To allow roll-back to continue, but at a slower rate than to the north and south, it seems likely that weak spots in the slab are present that allow to form pathways for mantle material to flow through. Segments where buoyancy anomalies such as the Juan Fernandez Ridge subduct may act as such weak zones: It resists roll-back more than denser adjacent lithosphere, creating tension and perhaps facilitate slab segmentation. Flat slabs as the Pampean flat slab may thus occur in those segments of the long Andean subduction zone where positive buoyancy may temporarily shallow the slab dip, and perhaps break the slab allowing mantle material to flow in from adjacent segments.

Enhanced positive buoyancy of the Nazca Ridge may also have aided the formation of the Peruvian flat slab (Gutscher et al. 2000; Pilger 1981). Interestingly, recent observations suggested that the Peruvian flat slab is breaking, indeed (Antonijevic et al. 2015). However, the width of the Peruvian flat slab segment is ~1500 km, three times as wide as the Pampean flat slab. Positive buoyancy of the Nazca Ridge alone may therefore insufficiently account for the

resistance in roll-back of the whole flat slab segment. We postulate that a potential additional cause of flat slab formation is the angle of the roll-back direction forced by absolute plate motion, which has an orientation approximately parallel to the trench (Fig. 2c). As recently shown (Chertova et al., 2014,) the rate of roll-back decreases with an increase of absolute velocity of a slab parallel to the trench. We therefore propose that the combination of positive buoyancy of the Nazca ridge as well as the absolute slab motion parallel to the trench resisted roll-back sufficiently to form the ~1500 km wide Peruvian flat slab segment.
Our straightforward kinematic analysis, with definitions of the terminology used in combination with our conceptual model (Fig. 2) provides first-order constraints on the long-debated formation of the Andean flat slab segments. We foresee that similar first-order constraints may be obtained on the evolution of the widely debated Laramide flat slab in the western US (DeCelles et al., 2009). Our research highlights that whereas the kinematic evolution of mountain belts can be analysed using a relative plate circuit, it is of key importance to study the geodynamics of subduction zones in a mantle reference frame.

Acknowledgements

First and above all I would like to thank Douwe van Hinsbergen, Wim Spakman and Lydian Boschman for their help, good discussions and reviewing my work. Furthermore I would like to thank Nadine McQuarrie who helped me in the start up phase of this project. My roommate Martha Kosters ensured that the whole project was a great experience and helped me with some good discussions.

References

Antonijevic, S.K. et al., 2015. The Role of Subducting Ridges in the Formation of Flat Slabs: Insights from the Peruvian Flat Slab. *EGU General Assembly 8671, held 78-17 April, 2015 in Vienna, Austria. id.1252*

Barazangi, M. & Isacks, B., 1976. Spatial distribution of earthquaktes and subduction of the Nasca plate beneath South America. *Geology*, 4(1971), pp.686–692.

Boschman, L. et al., 2014. Kinematic reconstruction of the Caribbean region since the Early Jurassic. *Earth Science Reviews*, 16, p.6829.

Boyden, J.A. et al., 2011. *Geoinformatics* G. R. Keller & C. Baru, eds., Cambridge: Cambridge University Press.

Cahill, T. & Isacks, B.L., 1992. Seismicity and shape of the subducted Nazca Plate. *Journal of Geophysical Research*, $^{3\,1}$, p.5^{1}947.

Chertova, M. V. et al., 2014. Geochemistry, Geophysics, Geosystems. , pp.3780–3792.

Cox, A. & Hart, R.B., 1986. Plate tectonics: how it works. *Plate tectonics: how it works.*

Doubrovine, P. V., Steinberger, B. & Torsvik, T.H., 2012. Absolute plate motions in a reference frame defined by moving hot spots in the Pacific, Atlantic, and Indian oceans. *Journal of Geophysical Research*, 55^{1} (B^{3}), p.$B4^{3}$545.

Eichelberger, N. & McQuarrie, N., 2015. Kinematic reconstruction of the Bolivian orocline. *Geosphere*, 55(6), pp.889–462.

Faccenda, M. & Capitanio, F.A., 2013. Seismic anisotropy around subduction zones: Insights from three-dimensional modeling of upper mantle deformation and SKS splitting calculations. *Geochemistry, Geophysics, Geosystems*, 14(1), pp.243–262.

Gutscher, M.A. et al., 2000. Geodynamics of flat subduction: Seismicity and tomographic constraints from the Andean margin. *Tectonics*, 19(5), pp.814–833.

Hayes, G.P., Wald, D.J. & Johnson, R.L., 2012. Slab1.0: A three-dimensional model of global subduction zone geometries. *Journal of Geophysical Research: Solid Earth*, 117(January), pp.1–15.

Van Hunen, J., van den Berg, A.P. & Vlaar, N.J., 2004. Various mechanisms to induce present-day shallow flat subduction and implications for the younger Earth: A numerical parameter study. *Physics of the Earth and Planetary Interiors*, 146, pp.179–194.

Jordan, T.E. et al., 1983. Andean tectonics related to geometry of subducted Nazca plate. *Geol. Soc. Am. Bull.*, [3] 8 (5[3 2] 7), pp. 785–361

Kley, J., Monaldi, C.R. & Salfity, J. a., 1999. Along-strike segmentation of the Andean foreland: causes and consequences. *Tectonophysics*, 301(1-2), pp.75–94.

Manea, V.C., Marta, P.G. & Manea, M., 2012. Chilean flat slab subduction controlled by overriding plate thickness and trench rollback. *Geology*, 40(1), pp.35–38.

O'Driscoll, L.J., Richards, M. a. & Humphreys, E.D., 2012. Nazca-South America interactions and the late Eocene-late Oligocene flat-slab episode in the central Andes. *Tectonics*, 31(2), pp.1 –16.

O'Neill, C., Müller, D. & Steinberger, B., 2005. On the uncertainties in hot spot reconstructions and the significance of moving hot spot reference frames. *Geochemistry, Geophysics, Geosystems*, [0] (8), p.n/a–n/a.

Oncken, O. et al., 2003. Deformation of the Central Andean Upper Plate System – Facts , Fiction , and Constraints for Plateau Models.

Pilger, R.H., 1981. Plate reconstructions, aseismic ridges, and low-angle subduction beneath the Andes. *Geological Society of America Bulletin*, 92(7), p.448.

Pindell, J.L. et al., 1988. A plate-kinematic framework for models of Caribbean evolution. *Tectonophysics*, 599(5-4), pp.121–138.

Ramos, V. a. & Folguera, a., 2009. Andean flat-slab subduction through time. *Geological Society, London, Special Publications*, 76[1] (5), pp.75–54.

Ramos, V.A., Cristallini, E.O. & Pe, D.J., 2002. The Pampean flat-slab of the Central Andes. *J. South Am. Earth Sci.*, 59 (6446), pp. 9[3] –78

Russo, R.M. & Silver, P.G., 1996. Cordillera formation, mantle dynamics, and the Wilson cycle. *Geology*, 68([0]), pp.955–514.

Schellart, W.P. et al., 2007. Evolution and diversity of subduction zones controlled by slab width. *Nature*, 446(March), pp.308–311.

Skinner, S.M. & Clayton, R.W., 2013. The lack of correlation between flat slabs and bathymetric impactors in South America. *Earth and Planetary Science Letters*, 371-372, pp.1–5.

Stern, C.R., 2004. Active Andean volcanism: its geologic and tectonic setting. *Revista geológica de Chile*, 75(6), pp.5^0 5–206.

Turcotte, D. & Schubert, G., 1982. *Geodynamics*.

Yáñez, G.A., Ranero, R. & Huene, V., 2001. Magnetic anomaly interpretation across the southern central ß The role of the Juan Fernandez Ridge in the late Tertiary evolution of the margin C6sar Diaz : -1400 km of the margin from From 11 Ma to present the collison point. , 106, pp.6325–6345.

Appendix I

Introduction

In this Appendix, we describe the kinematic restoration of the Andean fold-and-thrust belt that forms the basis of the analysis provided in the main paper. This has been done to determine the amount of shortening in the overriding plate and to reconstruct the trench relative to the mantle.

First, we give a hierarchy of the constraints used in our reconstruction. Next, we provide an overview of the study area and its subdivisions and a step-by-step reconstruction with the assumptions made to smooth the reconstruction and reduce discrepancies between regions.

Approach

The constraints that have been used for the kinematic reconstruction have been derived from shortening estimates from balanced cross sections, timing of deformation from thermochronology basin studies and intrusive contacts of plutons, rotations from paleomagnetic data and strike-slip displacements from geological mapping and seismologic data.

Shortening estimates based on balanced cross sections are the most certain data used in our reconstruction. A total of 50 transects has been used for the reconstruction of the several geomorphologic units and shortening directions have been reconstructed parallel on the transects when no vertical axis rotations were present.

Timing: Dating the timing of deformation has been done by a combination of thermochronologic data and basin studies. The cooling ages are estimated by $^{40}Ar/^{39}Ar$, zircon fission track, zircon (U-Th)/He, apatite fission track and apatite (U-Th)/He ages from across the Andes. It is especially a good indicator for the onset of deformation, but less good for the cessation of deformation.

Rotations: The main rotation patterns in the Central Andes are the counterclockwise rotation of the part north of the Arica bend and the clockwise rotations south of the Arica bend. Rotations near the Huancabamba bend (3-8 degrees S) have not been implemented in the reconstruction. The paleomagnetic data in the Andes is mainly taken from volcanic forearc rocks and not in the retroarc fold-thrust belt that have underwent deformation since ~50 Ma (Eichelberger & McQuarrie 2015). Therefore the paleomagnetic data has large uncertainties.

Transform faults: Displacements along strike-slip faults are the least well constrained source for our kinematic reconstruction. From geological and seismologic data it is known that the Cochabamba and the Rio Novillero Fault are left-lateral and right-lateral but a specific amount of displacement is unknown. The displacement and timing along the Magallanes-Fagnano fault

system are also still under debate. The proposed displacements are in the same order of magnitude (20-55 km) but the age of formation ranges from 100 to 7 Ma (Maffione et al. 2010 and references therein). Shortening estimates from the retroarc fold-thrust belt come from balanced cross-section These are sorted into ten different distinct geomorphologic regions in the Andean fold-thrust belt. The estimates for each region are listed in Table 1.
We use the freely available software package to make our reconstruction (http:// www.gplates.org) (Boyden et al. 2011). The Andean fold-thrust belt is divided into ten different geomorphologic units that are represented by the areas between different polylines. These lines move with respect to each other during deformation and change the area in between them. We reconstruct Andean deformation with respect to a fixed non-deforming South American foreland in the east.
Two rotation files are available in the auxiliary material, a rotation file purely based on the constraints and one that has been smoothed to decrease discrepancies between units.

General overview

The Andean fold-thrust can be divided in several geomorphic units (Figure 1) that were internally shortened by folding and thrusting. A total of 50 published balanced structural cross-sections were used to restore the deformation, an overview of the kinematic data derived from these can be found in Table 1.

From North to South, the Andes is subdivided in several segments, including the Colombian Andes, Ecuadorian Andes, Huancabamba bend, Peruvian Andes, Arica Bend, Bolivian Andes, Chilean Andes and Argentinean Andes. The Ecuadorian and the Colombian Andes, where interaction with the Caribean Plate occurred (Pindell et al. 1988; Bochman et al. 2014), have not been taken into account. In the south our reconstruction stops at the Scotia Sea and only takes into account the Magallanes fold-thrust belt on the Scotia Plate. We focus only on the system with merely overriding plate contraction.
Underneath the Peruvian and the Chilean Andes two segments of the Nazca Plate are subducting horizontally, respectively the Peruvian and Pampean flat slabs (Barazangi & Isacks 1976; Gutscher et al. 2000; Cahill & Isacks 1992; Hayes et al. 2012).

Along the Andes twelve different geomorphologic regions are identified (Kley et al. 1999). The largest shortening in the Andean fold-thrust belt was accommodated in the central part of the system, around the Arica bend. Here, the orogen can be divided in five geomorphic units, from west to east; the Western Cordillera; Altiplano-Puna plateau; Eastern Cordillera; Interandes; and the Subandes (Isaks 1988; Kley 1996).

The Western Cordillera is formed by the modern volcanic arc related to subduction of the Nazca Plate. Here, only minor deformation has been recognized and balanced cross sections of deformation in the basement of the arc are hard to construct due to the young volcanics that cover most of the region. Only two sections have attempted to take this deformation into account (sections 5, 7, Figure 2, Table 1).

The Western Cordillera is bounded to the east by the Altiplano-Puna plateau, which is a deformed intramontane basin with west-vergent thrusts covered by Neogene to recent sedimentary and volcanic rocks. The Altiplano plateau has its northern limit in southern Peru (Kley 1999). (Sections 9, 12, 15, 20, 21, Figure 2, Table1).

The Puna Plateau is the topographical continuation of the Altiplano Plateau and is also bounded by the Western and Eastern Cordillera. The cause of uplift of the plateau is still debated, on one side it is proposed that uplift is consistent with crustal shortening and on the other hand it is proposed that delamination of the eclogitic lower crust and lithosphere caused the uplift (Kay & Coira 2009 and references therein). At the surface Proterozoic and Paleozoic basement rocks are present as series of small mountains, Mesozoic sediments are present mainly at the eastern part of the plateau and cenozoic sediments and volcanics can be found in the intermontane basins (Coutand et al. 2001).

The Eastern Cordillera is the most prominent unit and has peak elevations of 6000 m and changes from a west-vergent style of backthrusting to an east-vergent style of fore-thrusting (McQuarrie 2002). It is composed of Cambrian to Devonian sedimentary rocks that are discontinuously overlain by Mesozoic and Cenozoic sedimentary and volcanic rocks (Müller et al. 2002). Within the Eastern Cordillera two strike-slip faults are active upon to today, the mainly E-W sinistral Cochabamba strike-slip fault and the N-S dextral Rio Novillero strike-slip fault (Eichelberger et al., 2013). However, displacement magnitudes along both faults are estimated.

The Interandes is an east-vergent thin-skinned fold-and-thrust belt consisting of Silurian through Mesozoic succession (Kley 1999).

The Subandes is an active east-vergent thin-skinned fold-and-thrust belt with partially blind thrusting and folding (Uba et al. 2009 and references therein). It composes of mostly Carboniferous to Neogene strata, with older rocks exposed locally (Kley 1999).

Towards the south the Andes can be divided into seven other geomorphic units; Santa Barbara System; Sierras Pampeanas ; Principal Cordillera; Frontal Cordillera; Precordillera; Patagonian Cordillera.

The Santa Barbara System is a continuation of the Subandes, characterized by mainly west verging, high angle thrust faults that involve basement rocks. The relationship of the thrust faults to location and thickness of cretaceous rocks suggests that these faults are inversed

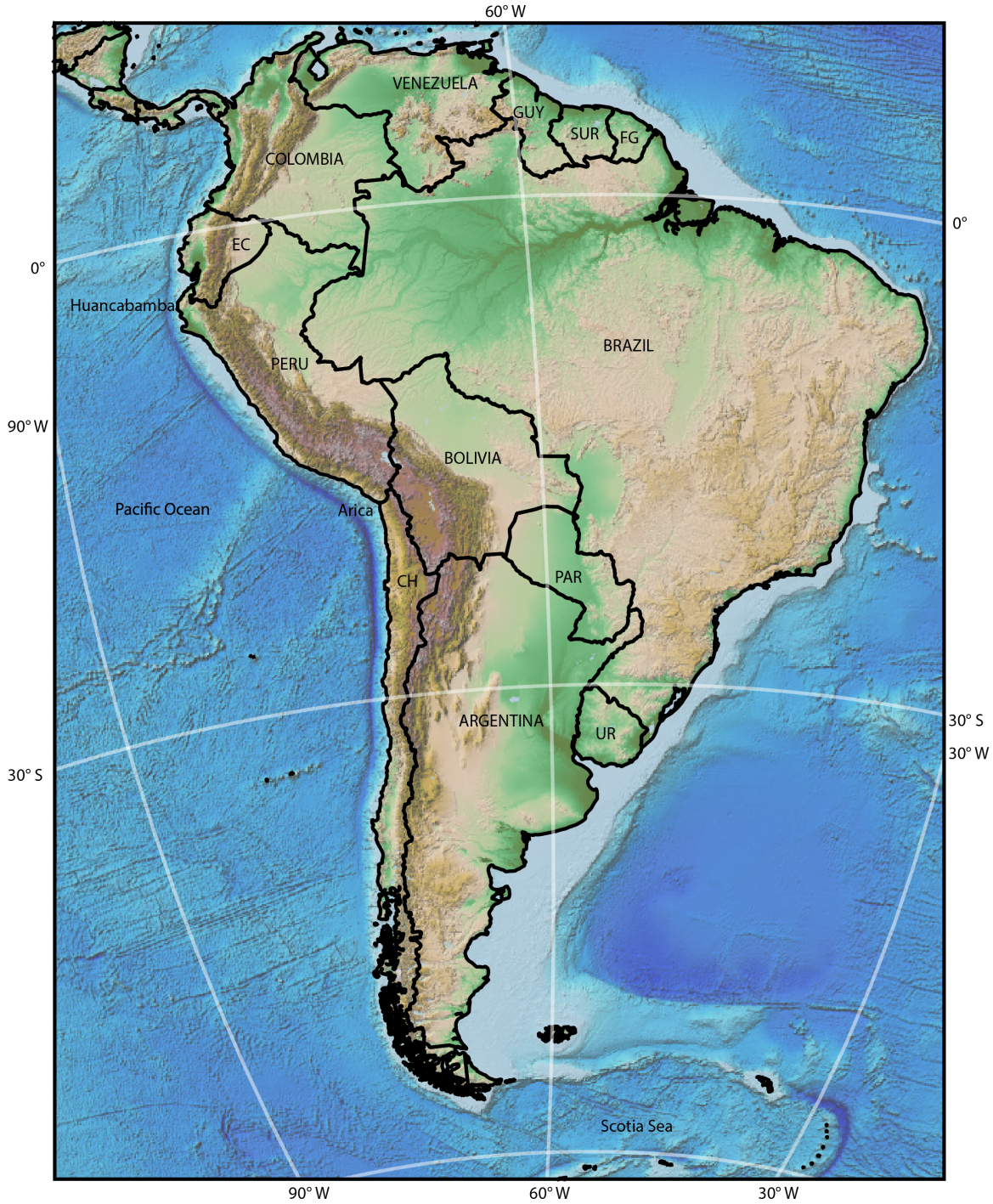

Figure 1: Geographic map (3D Globe projection) of South America. Huancabamba and Arica are two of the bends in the South American Plate Abbreviations are; CH, Chile; EC, Ecuador; FG, French Guiana; GUY, Guyana; PAR, Paraguay; SUR, Suriname; UR, Uruguay.

normal faults from a Cretaceous to Paleogene rift system. The Santa Barbara System was first considered part of the Subandes but due to the presence of thick Cretaceous strata and the reactivated normal faults it has been identified as a independent geological system (Kley et al., 1999 and references therein).

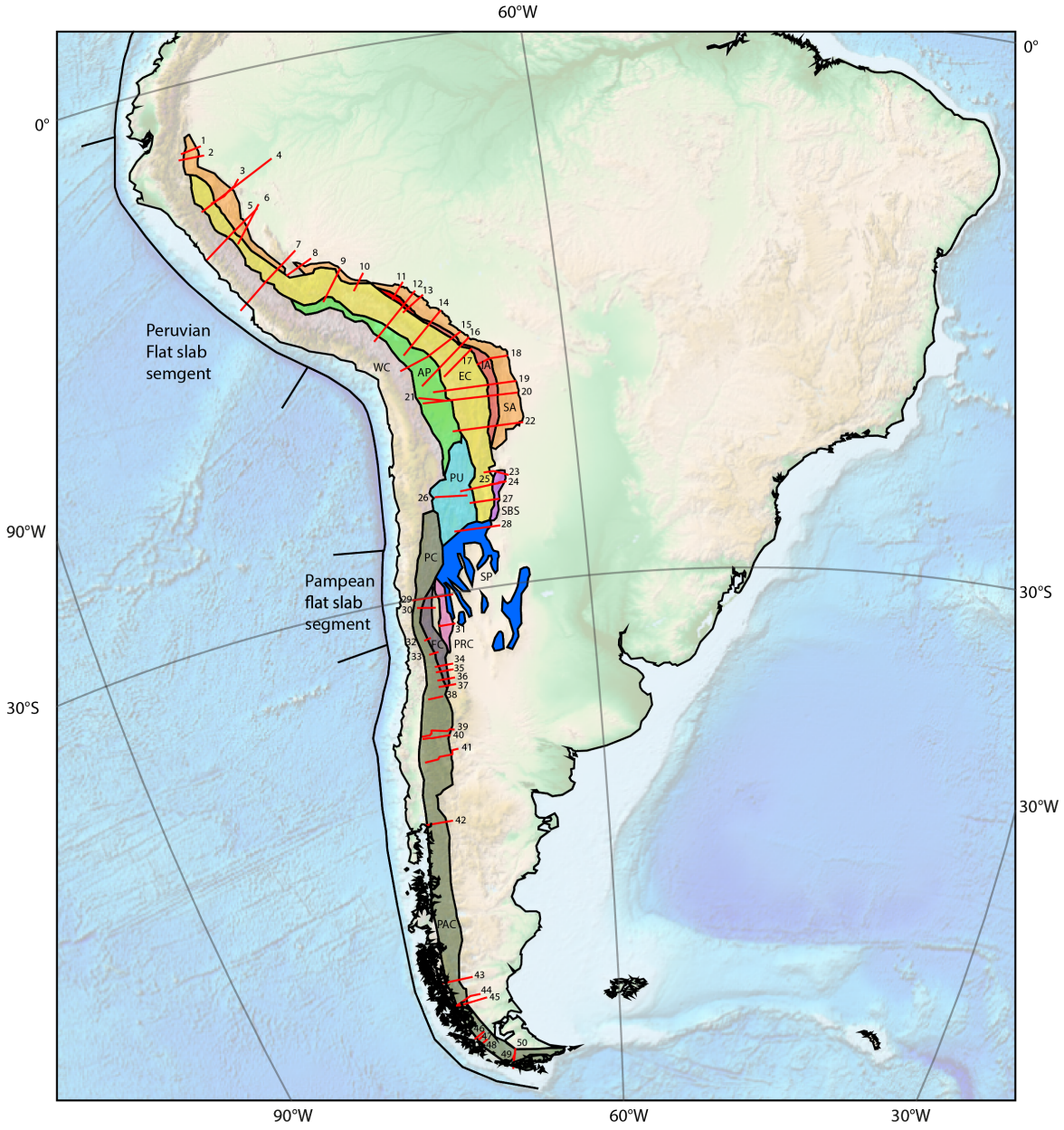

Figure 2: Tectonic map (3D Globe projection) of the Andes modified from Kley et al. (1999) and Eichelberger & McQuarrie (2015), showing the boundaries of deforming geomorphologic regions and the 50 transects used in the reconstruction. Abbreviations are WC, Western Cordillera; AP, Altiplano Plateau; EC, Eastern Cordillera; IA, Interandes; SA, Subandes; PU, Puna Plateau; SBS, Santa Barbara System; PC, Principal Cordillera; FC, Frontal Cordillera; PRC, Precordillera; SP, Sierras Pampeanas; PAC, Patagonian Cordillera.

The Sierras Pampaenas is a province of large wavelength basement uplifts and deep reaching thrust faults (Jordan & Allmendinger 1986). It is located in the region where the Naza Plate is subducting sub-horizontal.

The Principal Cordillera is located at the Chile – Argentina border and is a relatively long thin skinned mountain range and at some parts a thick skinned fold-and-thrust belt.

The Frontal Cordillera transits from the thin-skinned Principal Cordillera into a thick skinned fold-and-thrust belt with mainly east-verging faults.
The Precordillera is a thin-skinned thrust belt with west-verging structures and accounts for most of the shortening in this part of the Andes (Allmendinger et al. 1990). It is located above the Pampean flat slab segment of the Nazca Plate (Cahill & Isacks 1992; Barazangi & Isacks 1976). It consists of thick series of Early to Late Palaeozoic sediments, younger Mesozoic deposits can be found in the basin structures at the western and eastern boundaries (Von Gosen 1992).
The main fold-and-thrust belt of the Patagonian Cordillera is the thin-skinned Magallanes FTB, consisting of upper Cretaceous to Miocene sediments (Maffione et al. 2010 and references therein).
The Peruvian Andes has a total estimated shortening of 100 to 142 km, consisting of 53-80 km in the coastal belt and Western Cordillera (Sections 5 & 7), 26-46 km in the Eastern Cordillera (Sections 4, 5, 7 & 9) and 11-95 km in the Subandes (Sections 1-9). Timing of shortening is based on unconformities, intrusive contacts of plutons as observed in the field and AFT cooling ages (Pfiffner & Gonzalez 2013; Espurt et al. 2011).
The Bolivian Andes has a total estimated shortening of 277 to 380 km, consisting of 15-47 km in the Altiplano Plateau (Section 12, 15, 20 &21), 70-142 km in the Eastern Cordillera (Section 12, 14, 16-19, 22), 39-96 km in the Interandes (Section 12, 14, 16-19 & 22) and 60-86 km in the Subandes (Section 11-14, 16-19 & 22). Timing of shortening is based thermochronlogic data and basin studies (Eichelberger & McQuarrie 2015 and references therein)
South of the Bolivian Andes the Andean the total shortening is 117-163 km, consisting of 26 km in the Puna Plateau (Section 26), 70-95 km in the Eastern Cordillera (Section 24 & 27) and 21-30 km in the Santa Barbara System (Section 23-25)
At the position of the Pampean flat slab the Andean fold-and-thrust belt has a total shortening of 136 to 198 km, consisting of 30-60 km in the Principal Cordillera (Sections 29, 32, 33), 8-23 km in the Frontal Cordillera (30, 32-37), 88-95 km in the Precordillera (Sections 29, 31)and 10-20 km in the Sierras Pampeanas (Sections 28, 29).
Further down south the total shortening in the Andean fold-and-thrust belt is approximately equal to the amount of shortening in the Principal Cordillera and the Patagonian Cordillera (Sections 38-50).

Interpretation

Reconciling the kinematic constraints of Andean deformation (Table 1 and Figure 2) gives us the reconstruction of the Andean fold-and-thrust belt as shown in Figure 3. This reconstruction has been smoothened to decrease discrepancies between regions. An overview of the

Structure/ Region	Transect number	Type of data	Sense	Amount	Plate ID	Age	Reference
Subandes	1,2	Shortening estimate	ne-sw	11-20 km	2551	15-0 Ma	(Kley et al. 1998), after (Aleman & Marksteiner 1993) (Gil Rodriguez et al. 2001)
	3,4	Shortening estimate	ne-sw	84 -95 km	2553	23-0 Ma	(Hermoza et al. 2005; Eude 2014)
	5	Shortening estimate	ne-sw	24,7 km	2552	24-0 Ma	(Pfiffner & Gonzalez 2013)
	6,7	Shortening estimate	ne-sw	40-42,3 km	2546	24-0 Ma	(Kley et al. 1998), after (Koch 1962) (Pfiffner & Gonzalez 2013)
	8	Shortening estimate	ne-sw	57 km	2593	15-0 Ma	(Espurt et al. 2008)
	9,10	Shortening estimate	ne-sw	17 -20 km	2544	15-0 Ma	(Gotberg et al. 2009), (Kley et al. 1998) after (Sébrier et al. 1988) (Roeder 1988; Roeder & Chamberlain 1995)
	11,12,13	Shortening estimate	ne-sw	66 km	2539	15-0 Ma	(McQuarrie et al. 2008; Baby et al. 1989) (Roeder 1988; Roeder & Chamberlain 1995)
	14	Shortening estimate	ne-sw	66 km	2536	15-0 Ma	(McQuarrie et al. 2008)
	16	Shortening estimate	ne-sw	71 km	2533	10-0 Ma	(Barnes et al. 2012)
	17,18	Shortening estimate	ene-wsw	86 km	2528, 2530	15-0 Ma	(Eichelberger et al. 2013)
	19	Shortening estimate	e-w	67 km	2523	15-0 Ma	(Barnes et al. 2008)
	22	Shortening estimate	e-w	60-78 km	2519	15-0 Ma	(Uba et al. 2009; Echavarria et al. 2003)
		Paleomagnetic	counterclockwise	13 degrees	2530,2536 2539	15-0 Ma	(Arriagada et al. 2008)
		Paleomagnetic	counterclockwise	13 degrees	2533	10-0 Ma	(Arriagada et al. 2008)
		Paleomagnetic	clockwise	13 degrees	2519, 2523 2528	15-0 Ma	(Arriagada et al. 2008)
Eastern Cordillera	4	Shortening estimate	ne-sw	47 km	2549	30-23 Ma	(Eude 2014)
	5	Shortening estimate	ne-sw	26 km	2547	30-20 Ma	(Pfiffner & Gonzalez 2013)
	7	Shortening estimate	ne-sw	46 km	2554	30-20 Ma	(Pfiffner & Gonzalez 2013)
	9	Shortening estimate	ne-sw	91 km	2596	45-20 Ma	(Gotberg et al. 2009)
	15	Shortening estimate	ne-sw	123 km	2541	50-25 Ma	(McQuarrie et al. 2008)
	14	Shortening estimate	ne-sw	123 km	2538	50-25 Ma	(Barnes et al. 2006)

	16	Shortening estimate	ne-sw	142 km	2535	50-25 Ma	(Barnes et al. 2012)
	17,18	shortening estimate	ene-wsw	136 km	2532	50-25 Ma	(Eichelberger et al. 2013)
	19	shortening estimate	e-w	122 km	2525	40-20 Ma	(Barnes et al. 2008)
	22	shortening estimate	e-w	95 km	2522	40-20 Ma	(Ege et al. 2007)
	24	Shortening estimate	e-w	95 km	2521	40-20 Ma	(Pearson et al. 2013)
	27	Shortening estimate	e-w	70 km	2594	40-20 Ma	(Grier et al. 1991; Cristallini et al. 1997)
Interandes	12	Shortening estimate	e-w	48 km	2540	45-25 Ma	(McQuarrie et al. 2008)
	14	Shortening estimate	ne-sw	48 km	2537	45-25 Ma	(Gillis et al. 2006)
	16	Shortening estimate	ne-sw	39 km	2534	20-10 Ma	(Barnes et al. 2012)
	17,18	Shortening estimate	ene-wsw	43 km	2529,2531	45-15 Ma	(Eichelberger et al. 2013)
	19	Shortening estimate	e-w	96 km	2524	25-15 Ma	(Barnes et al. 2008)
	22	Shortening estimate	e-w	62 km	2520	20-10 Ma	(Ege et al. 2007)
Altiplano	9	shortening estimate	ne-sw	15 km	2597	15-0 Ma	(Gotberg et al. 2009)
	12	shortening estimate	ne-sw	40 km	2542	15-0 Ma	(McQuarrie et al. 2008)
	15	shortening estimate	ne-sw	47 km	2598	15-0 Ma	(McQuarrie 2002)
	15	shortening estimate	ne-sw	47 km	2587	15-0 Ma	(McQuarrie 2002)
	21	shortening estimate	e-w	24 km	2526	33-27 Ma	(Elger et al. 2005)
	20	shortening estimate	ne-sw	41 km	2526	15-0 Ma	(McQuarrie 2002)
Precordillera	29	Shortening estimate	e-w	95 km	2505	13-0 Ma	(Allmendinger et al. 1990), (Allmendinger & Judge 2014)
	31	Shortening estimate	e-w	88 km	2505	13-0 Ma	(Von Gosen 1992; Allmendinger & Judge 2014)
Principal Cordillera	29	Shortening estimate	e-w	<30 km	2513	20-8,6 Ma	(Allmendinger et al. 1990; Ramos et al. 2002)
	32,33	Shortening estimate	e-w	55-60 km	2511	20-8,6 Ma	(Ramos et al. 1996; Ramos et al. 2002)
	38	Shortening estimate	e-w	73 km	2507	20-8,6 Ma	(Ramos et al. 1996; Ramos et al. 2002)
	39	Shortening estimate	e-w	29,5 km	2591	11,6-0 Ma	(Rojas Vera et al. 2014)
	39	extension	e-w	3 km	2591	33,9-16 Ma	(Rojas Vera et al. 2014)
	40,41	Shortening estimate	e-w	5,9-12,5 km	2589	100,5-56 Ma	(Rojas Vera et al. 2014)
	40,41	extension	e-w	0,8-1 km	2589	56-11,6 Ma	(Rojas Vera et al. 2014)
	40,41	Shortening estimate	e-w	5,3-13,2 km	2589	11,6-0 Ma	(Rojas Vera et al. 2014)

	42	Shortening estimate	e-w	24 km	2502	11,6-0 Ma	(Kley et al. 1999; Rojas Vera et al. 2014)
Frontal Cordillera	30	Shortening estimate	e-w	8 km	2518	8,5-4 Ma	(Heredia 2002)
	32,33	Shortening estimate	e-w	18 km	2510	8,5-4 Ma	(Ramos et al. 1996)
	34,35	Shortening estimate	e-w	15-23 km	2509	8,5-4 Ma	(Giambiagi et al. 2012; Giambiagi & Ramos 2002)
	36,37	Shortening estimate	e-w	8 km	2506	7,7-4 Ma	(Giambiagi et al. 2012)
Santa Barbara System	23	Shortening estimate	e-w	30 km	2517	26,7 Ma	(Kley & Monaldi 2002; Ege et al. 2007)
	24,25	Shortening estimate	e-w	21 km	2517	26,7 Ma	(Kley & Monaldi 2002; Ege et al. 2007) (Pearson et al. 2013)
Puna	26	Shortening estimate	e-w	37 km	2522	37,8-0 Ma	(Coutand et al. 2001)
Patagonian Cordillera	43	Shortening estimate	e-w	35 km	2586	23-5,3 Ma	(Kraemer 1998)
	44	Shortening estimate	e-w	24 km	2585	23-5,3 Ma	(Ghiglione et al. 2014)
	45	Shortening estimate	ne-sw	27 km	2584	88-74 Ma	(Fosdick et al. 2011)
	45	Shortening estimate	ne-sw	6.1 km	2584	74-27 Ma	(Fosdick et al. 2011)
	45	Shortening estimate	ne-sw	3.4 km	2584	27-21 Ma	(Fosdick et al. 2011)
	45	Shortening estimate	ne-sw	2.2 km	2584	21-18 Ma	(Fosdick et al. 2011)
	45	Shortening estimate	ne-sw	0.9 km	2584	18-0 Ma	(Fosdick et al. 2011)
	46,47,48	Shortening estimate	ne-sw	23 km (25.9%)	2583	84-33,9 Ma	(Betka & Klepeis 2013)
	49,50	Shortening estimate	n-s	50-83 km	2581	66-0 Ma	(Kley et al. 1999; Klepeis et al. 2010)
Sierras Pampeanas	28	Shortening estimate	e-w	20 km	2504	5-0 Ma	(Allmendinger 1986; Jordan & Allmendinger 1986)
	29	Shortening estimate	e-w	10-20 km	2504	5-0 Ma	(Ramos et al. 1996)
Magallanes-Fagnano Fault system		Strike slip	left lateral	50 km		8-0 Ma	(Torres-Carbonell et al. 2008)
Western Cordillera and coastal belt	5	Shortening estimate	Ne-sw	52,5 km	2555	50-0 Ma	(Pfiffner & Gonzalez 2013)
	7	Shortening estimate	Ne-sw	80 km	2548	50-0 Ma	(Pfiffner & Gonzalez 2013)

			~31 km	2527, 2516	20-0 Ma	
	Between 22-27	Subduction erosion				(Kukowski & Oncken 2006; von Huene 2003;
			~40 km	2514	15-0 Ma	Scheuber & Bogdanic 1994)
	29	Subduction erosion	~40 km	2512	10-0 Ma	(Stern 1991)
Subduction erosion	33	Subduction erosion	~10 km	2503	11-3 Ma	(Kukowski & Oncken 2006)
	41	Subduction erosion				(Kukowski & Oncken 2006)

Table 1: Displacements used in this reconstruction

assumptions made can be found underneath per geomorphologic region that has been smoothened.

Eastern Cordillera: We reconstructed a 84 degrees clockwise rotation of the Eastern Cordillera at 13-14 degrees S between 45-20 Ma. This avoids the appearance of a left lateral strike-slip fault within the Eastern Cordillera to the north and is consistent with large counterclockwise rotations in the forearc of Southern Peru (Roperch et al. 2006). Displacements of the Cochabamba Fault and the Rio Novillero Fault in the Eastern Cordillera are not exactly known. In our model we have used the preferred values from Eichelberger & McQuarrie (2015). The left lateral strike slip Cochabamba Fault had a displacement of 50 km from 25-0 Ma and the right lateral strike slip Rio Novillero Fault had a displacement of less than 10 km from 15-0 Ma. The timing of deformation for the Eastern at transect 14 has been estimated at 45-20 and 15-0 Ma by thermo chronological data (Barnes et al. 2006), though in our reconstruction we assume that deformation occurred between 50-25 Ma following the reconstruction of Eichelberger & McQuarrie (2015). We assume the same deformation time for the transects 15 and 16 where the estimated time of deformation was between 55-21 Ma (Barnes et al. 2012).

Interandes: The reconstruction of the central part of the Andes by Eichelberger & McQuarrie (2015) has been used as a base for my reconstruction of the Interandes, this includes the timing of deformation for transects 14,16,17,18,19 and 22. These were respectively from north to south; before 25 and 18-5 Ma; 18-6 Ma; 42-18 Ma; 42-18 Ma; 22-19 Ma; and 18-9 Ma (Gillis et al. 2006; Barnes et al. 2012; Eichelberger et al. 2013; Barnes et al. 2008; Ege et al. 2007) and have been assumed to be; 45-25 Ma; 20-10 Ma; 45-15 Ma; 45-15 Ma; 25-15 Ma; and 20-10 Ma. The other adjustment made was 59 km of extra shortening from 45-15 Ma for the Interandes at transect 15.

Subandes: Timing of deformation in the Subandes at transect 5^0 has been estimated on 54-5 Ma (Barnes et al. 2012), we assume this to be 10-0 Ma because deformation in the Subandes is still ongoing (Brooks et al. 2011). At transect 22 the estimated time of deformation was 10-0 Ma (Uba et al. 2009), in the reconstruction this is assumed to be 15-0 Ma.
Following the reconstruction of Eichelberger & McQuarrie (2015) we assume that the rotations in the Central Andes are related to Subandean deformation and therefore start at 15 and is still ongoing.

Puna: The amount of shortening estimates for the Puna Plateau was relatively low and therefore 37 km of shortening (Coutand et al. 2001) has been used for the entire Puna Plateau.

Principal Cordillera: The most northern part of the Principal Cordillera had no constraints on shortening estimates. We therefore chose to let the most northern part follow the motions of the Puna Plateau so that there would not be any extension between the Principal Cordillera and the Puna Plateau.

Patagonian Cordillera: The Patagonian Cordillera at transects 8^0-48 has minor shortening compared to the north and south so an extra amount of 37 km shortening from 33,9-8 Ma has been estimated to account for this differences. At transects 44 and 45 another 15 km of extra shortening has been estimated from 22-0 Ma.

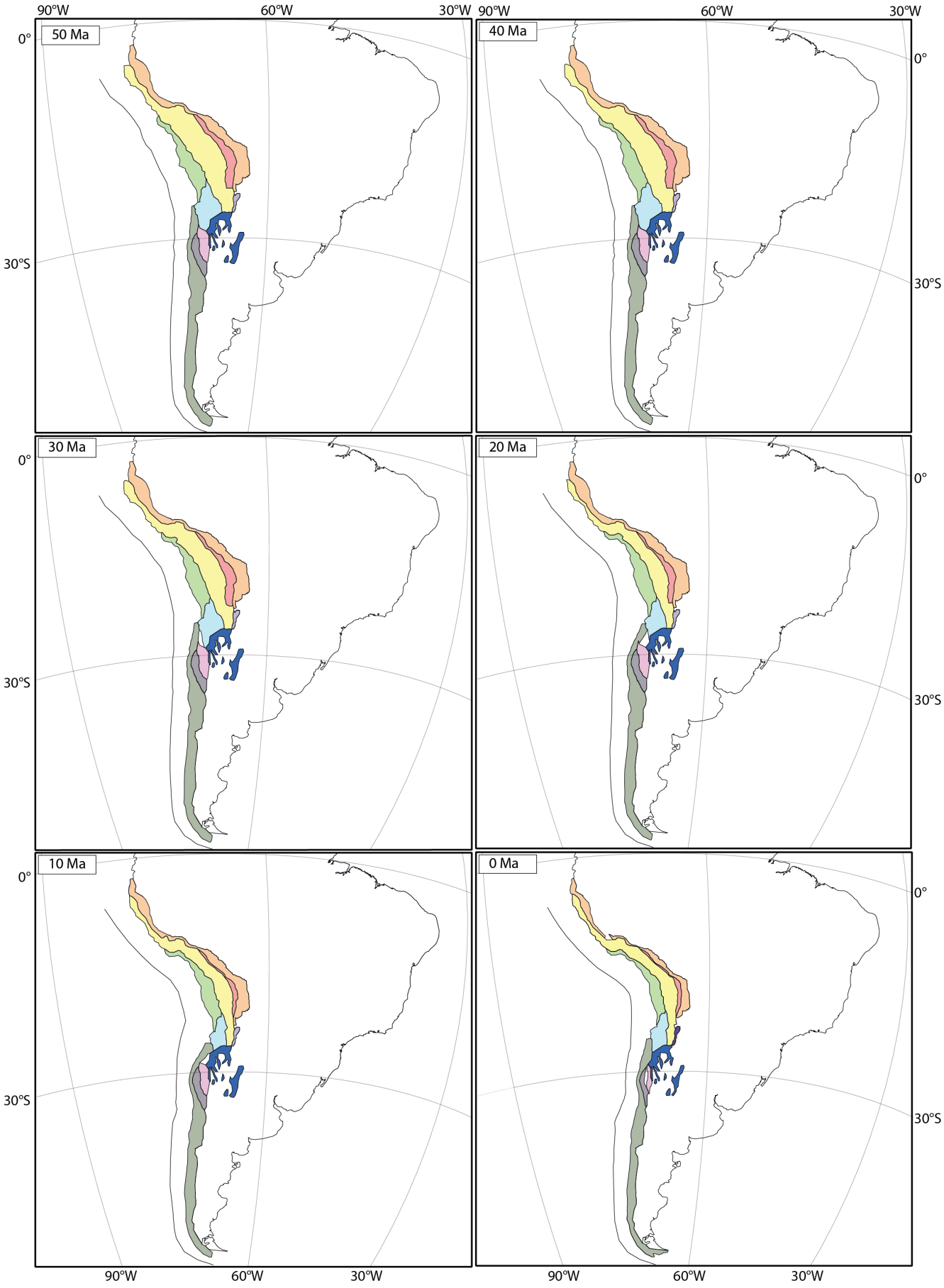

Figure 3: Reconstruction of the Andean deformation at 50, 40, 30, 20, 10 and 0 Ma with South America fixed

Appendix II

Introduction

To determine if previous stages of slab flattening could have occurred due to subduction of a locally thickened oceanic crust, we need to find conjugates on the Pacific Plate. First we searched for island arcs or plateaus like the Marquesas, Tuamotu, Austral and Manihiki Plateaus. When a mid ocean ridge started to develop we created a conjugate of the plateau on the Farallon Plate. The moment of flat slab subduction of former flat slab regions underneath South America is known (Ramos & Folguera 2009). By comparing the place of arrival at the trench of the conjugates and the onset of flattening we could determine whether a locally thickened crust could have caused the slab to flatten.

Conjugates on the Pacific Plate

At 120,4 Ma along the eastern margin of the Manihiki Plateau a mid ocean ridge developed which could have separated a part of the Manihiki Plateau. This conjugate part has been reconstructed with a width of ~220 km width and a 950 km length. At 83,5 Ma a new mid ocean ridge developed at the place of the Manihiki conjugate, from this point in time its motion is related to that of the Farallon Plate. At 34 Ma the conjugate reaches the trench and starts to subducts underneath South America (Fig. 4).

The conjugates of the Marquesas, Tuamotu and Austral Plateaus/Chains are the Inca Plateau (Gutscher et al. 1999), the Nazca Ridge and the Iquique Ridge. The Inca Plateau arrives at the trench at ~17 Ma, however it has a present location of 600 km more eastward than was proposed (Gutscher et al. 1999), which has also been mentioned by Skinner & Clayton (2013). The Nazca Ridge arrives at the trench around ~13 Ma which is consistent with work from Hampel (2002) (Fig. 5).

We also reconstructed conceptual plateaus consistent with the time and place of the former flat slabs. We reconstructed their motion back in time to see if a conjugate of these conceptual plateaus would match with present plateaus or other anomalies on the Pacific Plate.

Conclusions

In Figure 4 the position of the former Altiplano, Puna and Payenia flat slab regions are presented and as can be seen the conjugate feature of the Manihiki Plateau does not correspond with one of these flat slab regions. Also the Inca Plateau which has been proposed to account for the western part of the Peruvian flat slab (Gutscher et al. 1999) has already been

subducted to greater depths. Thus, it cannot form a resistance to subduction anymore. Creating conceptual plateaus on the locations of the former flat slab regions did not lead to the recognition of possible missed volcanic chains or plateaus.

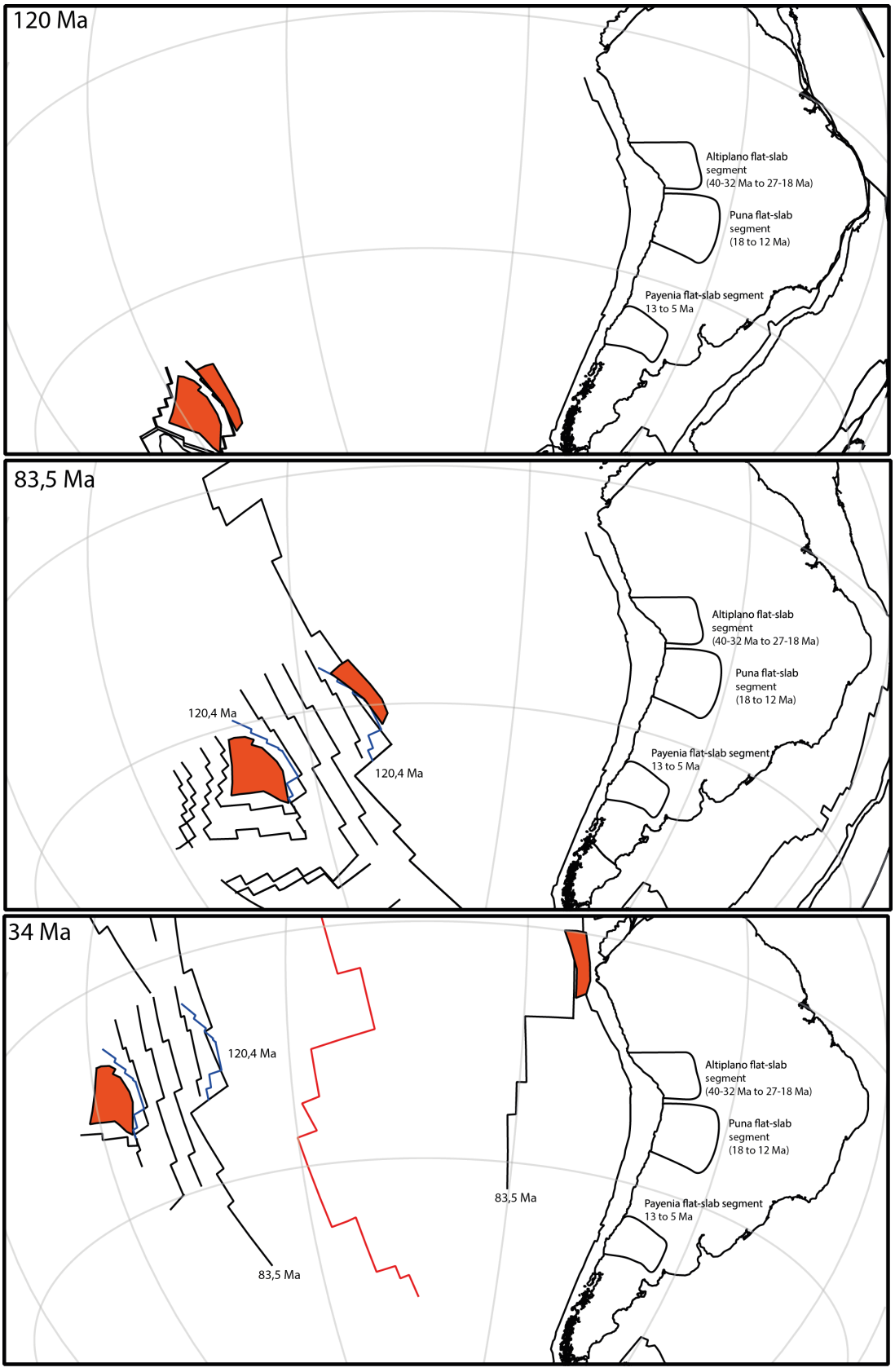

Figure 4: The position of the Manihiki and its conjugate feature at 120, 83.5 and 34 Ma with South America fixed. The Manihiki Plateau and its conjugate feature on the Farallon Plate are presented in orange. The regions of the former flat slab regions are projected with their moment of appearance (Ramos & Folguera, 2009)

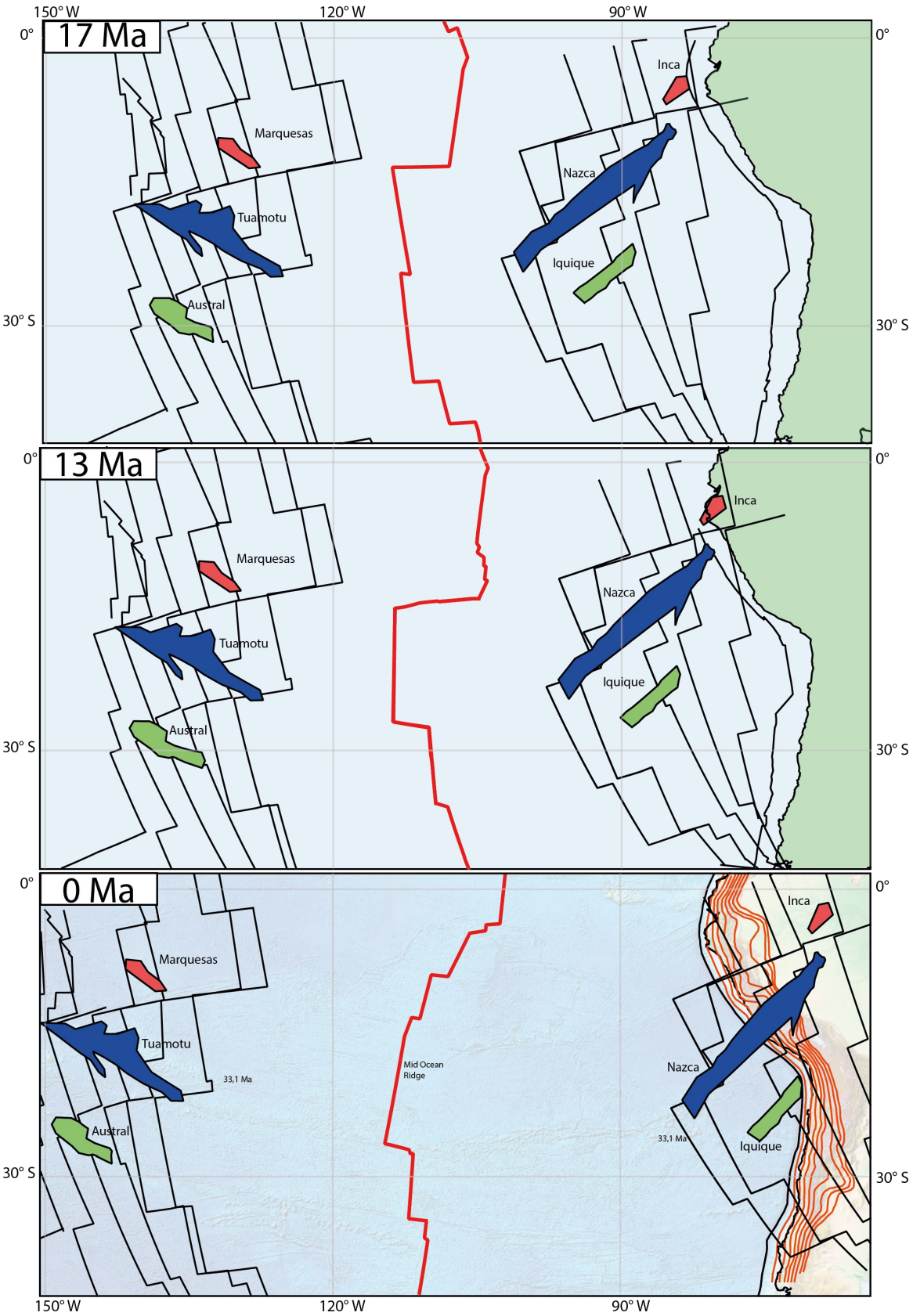

Figure 5: Location of the Marquesas; Tuamotu; Austral; Inca; Nazca; and Iquique Ridges and Plateaus for 17, 13 and 0 Ma with South America fixed. Note that the both the Inca and Nazca Ridge have already passed the 120 km depth line and therefore must have subducted to greater depths.

References

Aleman, A. & Marksteiner, R., 1993. Structural styles in the Santiago fold and thrust belt, Peru: A salt related orogenic belt. Available at: http://www.documentation.ird.fr/hor/fdi:38392 [Accessed June 18, 2015].

Allmendinger, R.W. et al., 1990. Foreland shortening and crustal balancing in the Andes at 30 S Latitude. , 9(4), pp.789–809.

Allmendinger, R.W., 1986. Tectonic development , southeastern border of the Puna Plateau , northwestern Tectonic development , southeastern border of the Puna Plateau , northwestern Argentine Andes.

Allmendinger, R.W. & Judge, P. a., 2014. The Argentine Precordillera: A foreland thrust belt proximal to the subducted plate. *Geosphere*, 10(6), pp.1203–1218. Available at: http://geosphere.gsapubs.org/cgi/doi/10.1130/GES01062.1 [Accessed December 9, 2014].

Arriagada, C. et al., 2008. Paleogene building of the Bolivian Orocline: Tectonic restoration of the central Andes in 2-D map view. *Tectonics*, 27(6), p.n/a–n/a. Available at: http://doi.wiley.com/10.1029/2008TC002269 [Accessed October 17, 2014].

Baby, P., Hérail, G. & Lopez, J., 1989. Structure de la zone subandine de Bolivie: influence de la géométrie des séries sédimentaires antéorogéniques sur la propagation des chevauchements. *CR Acad. Sci. …*. Available at: http://horizon.documentation.ird.fr/exl-doc/pleins_textes/pleins_textes_5/b_fdi_23-25/31118.pdf [Accessed June 18, 2015].

Barazangi, M. & Isacks, B., 1976. Spatial distribution of earthquaktes and subduction of the Nasca plate beneath South America. *Geology*, 4(1971), pp.686–692.

Barnes, J.B. et al., 2006. Eocene to recent variations in erosion across the central Andean fold-thrust belt, northern Bolivia: Implications for plateau evolution. *Earth and Planetary Science Letters*, 68^2 (5-2), pp.118–133. Available at: http://linkinghub.elsevier.com/retrieve/pii/S0012821X06003712 [Accessed October 21, 2014].

Barnes, J.B. et al., 2012. Linking orography, climate, and exhumation across the central Andes. *Geology*, 84(56), pp.5579–1138. Available at: http://geology.gsapubs.org/cgi/doi/10.1130/G33229.1 [Accessed October 25, 2014].

Barnes, J.B. et al., 2008. Thermochronometer record of central Andean Plateau growth, Bolivia (19.5°S). *Tectonics*, 27(3), p.n/a–n/a. Available at: http://doi.wiley.com/10.1029/2007TC002174 [Accessed October 25, 2014].

Betka, P.M. & Klepeis, K., 2013. Structure of the Patagonian fold-thrust belt in the Magallanes region of Chile , 53 ° - 55 ° S Lat .

Bochman, L. et al., 2014. Kinematic reconstruction of the Caribbean region since the Early Jurassic. *Earth Science Reviews*, 16, p.6829. Available at: http://dx.doi.org/10.1016/j.earscirev.2014.08.007.

Boyden, J.A. et al., 2011. *Geoinformatics* G. R. Keller & C. Baru, eds., Cambridge: Cambridge University Press. Available at: http://www.scopus.com/inward/record.url?eid=2-s2.0-84928086845&partnerID=tZOtx3y1 [Accessed June 11, 2015].

Brooks, B. a. et al., 2011. Orogenic-wedge deformation and potential for great earthquakes in the central Andean backarc. *Nature Geoscience*, 4(6), pp.380–383. Available at: http://dx.doi.org/10.1038/ngeo1143.

Cahill, T. & Isacks, B.L., 1992. Seismicity and shape of the subducted Nazca Plate. *Journal of Geophysical Research*, $^{3\,1}$, p.5^{1}947.

Coutand, I. et al., 2001. Style and history of Andean deformation, Puna plateau, northwestern Argentina. *Tectonics*, 20(2), pp.210–234. Available at: http://doi.wiley.com/10.1029/2000TC900031.

Cristallini, E., Cominguez, A.H. & Ramos, V.A., 1997. Deep structure of the Metan-Guachipas region: tectonic inversion in Northwestern Argentina. *Journal of South American Earth Sciences*, 54(9-6), pp.403–421. Available at: http://www.scopus.com/inward/record.url?eid=2-s2.0-0031370893&partnerID=tZOtx3y1 [Accessed May 29, 2015].

Echavarria, L. et al., 2003. Subandean thrust and fold belt of northwestern Argentina : Geometry and timing of the Andean evolution. , 6(6), pp.965–985.

Ege, H. et al., 2007. Exhumation history of the southern Altiplano plateau (southern Bolivia) constrained by apatite fission track thermochronology. *Tectonics*, 26(1), p.n/a–n/a. Available at: http://doi.wiley.com/10.1029/2005TC001869 [Accessed October 25, 2014].

Eichelberger, N. et al., 2013. New constraints on the chronology, magnitude, and distribution of deformation within the central Andean orocline. *Tectonics*, 32(5), pp.1432–1453. Available at: http://doi.wiley.com/10.1002/tect.20073 [Accessed November 4, 2014].

Eichelberger, N. & McQuarrie, N., 2015. Kinematic reconstruction of the Bolivian orocline. *Geosphere*, 55(6), pp.889–462. Available at: http://geosphere.gsapubs.org/cgi/doi/10.1130/GES01064.1.

Elger, K., Oncken, O. & Glodny, J., 2005. Plateau-style accumulation of deformation: Southern Altiplano. *Tectonics*, 24(4), p.n/a–n/a. Available at: http://doi.wiley.com/10.1029/2004TC001675 [Accessed November 11, 2014].

Espurt, N. et al., 2011. A scenario for late Neogene Andean shortening transfer in the Camisea Subandean zone (Peru, 12 S): Implications for growth of the northern Andean Plateau. *Geological Society of America Bulletin*, 567(^{3}-10), pp.2050–2068. Available at: http://gsabulletin.gsapubs.org/cgi/doi/10.1130/B30165.1 [Accessed October 22, 2014].

Espurt, N. et al., 2008. Paleozoic structural controls on shortening transfer in the Subandean foreland thrust system, Ene and southern Ucayali basins, Peru. *Tectonics*, 27(3), p.n/a–n/a. Available at: http://doi.wiley.com/10.1029/2007TC002238 [Accessed October 22, 2014].

Eude, A., 2014. Adrien Eude To cite this version:

Fosdick, J.C. et al., 2011. Kinematic evolution of the Patagonian retroarc fold-and-thrust belt and Magallanes foreland basin, Chile and Argentina, 51 30'S. *Geological Society of America Bulletin*, 567(^{3}-10), pp.1679–1698. Available at: http://gsabulletin.gsapubs.org/cgi/doi/10.1130/B30242.1 [Accessed October 13, 2014].

Ghiglione, M.C. et al., 2014. Geodynamic context for the deposition of coarse-grained deep-water axial channel systems in the Patagonian Andes. *Basin Research*, 26(6), pp.726–745. Available at: http://doi.wiley.com/10.1111/bre.12061 [Accessed January 7, 2015].

Giambiagi, L. et al., 2012. Thrust belts of the southern Central Andes: Along-strike variations in shortening, topography, crustal geometry, and denudation. *Geological Society of America Bulletin*, 568(^{1}-8), pp.1339–1351. Available at: http://gsabulletin.gsapubs.org/cgi/doi/10.1130/B30609.1 [Accessed November 25, 2014].

Giambiagi, L.B. & Ramos, V.A., 2002. Structural evolution of the Andes in a transitional zone between ¯ at and. , 15.

Gil Rodriguez, W., Baby, P. & Ballard, J.-F., 2001. Structure et contrôle paléogéographique de la zone subandine péruvienne. *Comptes Rendus de l'Académie des Sciences - Series IIA -*

Earth and Planetary Science, 777(55), pp.[1] 85–748. Available at: http://linkinghub.elsevier.com/retrieve/pii/S1251805001016937.

Gillis, R.J., Horton, B.K. & Grove, M., 2006. Thermochronology, geochronology, and upper crustal structure of the Cordillera Real: Implications for Cenozoic exhumation of the central Andean plateau. *Tectonics*, 25(6), p.n/a–n/a. Available at: http://doi.wiley.com/10.1029/2005TC001887 [Accessed October 25, 2014].

Von Gosen, W., 1992. Structural evolution of the Argentine Precordillera : the Rio San Juan section to result from a subduction process of the Palaeo-Pacific. , 14(6).

Gotberg, N., McQuarrie, N. & Caillaux, V.C., 2009. Comparison of crustal thickening budget and shortening estimates in southern Peru (12-14 S): Implications for mass balance and rotations in the "Bolivian orocline." *Geological Society of America Bulletin*, 122(5-6), pp.727–742. Available at: http://gsabulletin.gsapubs.org/cgi/doi/10.1130/B26477.1 [Accessed October 22, 2014].

Grier, M.E., Salfity, J. a. & Allmendinger, R.W., 1991. Andean reactivation of the Cretaceous Salta rift, northwestern Argentina. *Journal of South American Earth Sciences*, 4(4), pp.351–372. Available at: http://linkinghub.elsevier.com/retrieve/pii/0895981191900078.

Gutscher, M. a. et al., 1999. The "lost Inca Plateau": Cause of flat subduction beneath Peru? *Earth and Planetary Science Letters*, 5[1] 5(7), pp.779–341.

Gutscher, M.A. et al., 2000. Geodynamics of flat subduction: Seismicity and tomographic constraints from the Andean margin. *Tectonics*, 19(5), pp.814–833.

Hampel, A., 2002. The migration history of the Nazca Ridge along the Peruvian active margin: A re-evaluation. *Earth and Planetary Science Letters*, 203, pp.665–679.

Hayes, G.P., Wald, D.J. & Johnson, R.L., 2012. Slab1.0: A three-dimensional model of global subduction zone geometries. *Journal of Geophysical Research: Solid Earth*, 117(January), pp.1–15.

Heredia, N., 2002. Geological setting of the Argentine Frontal Cordillera in the ¯ at-slab. , 15, pp.79–99.

Hermoza, W. et al., 2005. The Huallaga foreland basin evolution: Thrust propagation in a deltaic environment, northern Peruvian Andes. *Journal of South American Earth Sciences*, 19(1), pp.21–34. Available at: http://linkinghub.elsevier.com/retrieve/pii/S0895981105000544 [Accessed October 27, 2014].

Von Huene, R., 2003. Subduction erosion and basal friction along the sediment-starved convergent margin off Antofagasta, Chile. *Journal of Geophysical Research*, 108(B2).

Isaks, B.L., 1988. Uplift of the Central Andean Plateau and bending of the Bolivian orocline. , 93.

Jordan, T.E. & Allmendinger, R.W., 1986. The Sierras Pampeanas of Argentina: A modern analogue of Rocky Mountain foreland deformation.

Kay, S.M. & Coira, B.L., 2009. lithospheric loss , magmatism , and crustal fl ow under the central Andean Altiplano-Puna Plateau. *Geological Society of America Memoir*, 204(November), pp.1–32.

Klepeis, K. et al., 2010. Continental underthrusting and obduction during the Cretaceous closure of the Rocas Verdes rift basin, Cordillera Darwin, Patagonian Andes. *Tectonics*, 29 (3), p.n/a–n/a. Available at: http://doi.wiley.com/10.1029/2009TC002610 [Accessed December 3, 2014].

Kley, J., 1999. Geologic and geometric constraints on a kinematic model of the Bolivian orocline. *Journal of South American Earth Sciences*, 56(6), pp.665–235. Available at: http:// linkinghub.elsevier.com/retrieve/pii/S0895981199000152.

Kley, J. et al., 1998. Tectonic shortening and crustal thickness in the Central Andes : How good is the correlation ?

Kley, J., 1996. Transition from basement-involved to thin-skinned thrusting in the Cordillera Oriental of southern Bolivia. *Tectonics*, 15(4), p.763.

Kley, J. & Monaldi, C.R., 2002. Tectonic inversion in the Santa Barbara System of the central Andean foreland thrust belt, northwestern Argentina. *Tectonics*, 21(6), pp.11–1–11–18. Available at: http://doi.wiley.com/10.1029/2002TC902003 [Accessed October 24, 2014].

Kley, J., Monaldi, C.R. & Salfity, J. a., 1999. Along-strike segmentation of the Andean foreland: causes and consequences. *Tectonophysics*, 301(1-2), pp.75–94. Available at: http:// linkinghub.elsevier.com/retrieve/pii/S0040195198902232.

Koch, E., 1962. Die Tektonik im Subandin des Mittel-Ucayali-Gebietes, Ostperu. Available at: https://scholar.google.nl/scholar?q=koch+1962+Die+Tektonik+im+Subandin+des+Mittel-Ucayali-+Gebietes&btnG=&hl=nl&as_sdt=0%2C5#0 [Accessed June 18, 2015].

Kraemer, P.E., 1998. Structure of the Patagonian Andes: Regional Balanced Cross Section at 50° S, Argentina. *International Geology Review*, 40(10), pp.896–915. Available at: http://

www.tandfonline.com/doi/abs/10.1080/00206819809465244 [Accessed January 7, 2015].

Kukowski, N. & Oncken, O., 2006. Subduction Erosion – the " Normal " Mode of Fore-Arc Material Transfer along the Chilean Margin ? *The Andes*, pp.217–236.

Maffione, M. et al., 2010. Paleomagnetic evidence for a pre-early Eocene (~50Ma) bending of the Patagonian orocline (Tierra del Fuego, Argentina): Paleogeographic and tectonic implications. *Earth and Planetary Science Letters*, 289(1-2), pp.273–286. Available at: http://linkinghub.elsevier.com/retrieve/pii/S0012821X09006621 [Accessed October 29, 2014].

McQuarrie, N., 2002. The kinematic history of the central Andean fold-thrust belt, Bolivia: Implications for building a high plateau. *Bulletin of the Geological Society of America*, 114 (8), pp.950–963.

McQuarrie, N., Barnes, J.B. & Ehlers, T.A., 2008. Geometric, kinematic, and erosional history of the central Andean Plateau, Bolivia (15-17°S). *Tectonics*, 27(3), p.n/a–n/a. Available at: http://doi.wiley.com/10.1029/2006TC002054 [Accessed October 21, 2014].

Müller, J.P., Kley, J. & Jacobshagen, V., 2002. Structure and Cenozoic kinematics of the Eastern Cordillera, southern Bolivia (21°S). *Tectonics*, 21(5).

Pearson, D.M. et al., 2013. Influence of pre-Andean crustal structure on Cenozoic thrust belt kinematics and shortening magnitude: Northwestern Argentina. *Geosphere*, 9(6), pp.1766 –1782. Available at: http://geosphere.gsapubs.org/cgi/doi/10.1130/GES00923.1 [Accessed October 8, 2014].

Pfiffner, O. & Gonzalez, L., 2013. Mesozoic–Cenozoic Evolution of the Western Margin of South America: Case Study of the Peruvian Andes. *Geosciences*, 3(2), pp.262–310. Available at: http://www.mdpi.com/2076-3263/3/2/262/ [Accessed November 26, 2014].

Pindell, J.L. et al., 1988. A plate-kinematic framework for models of Caribbean evolution. *Tectonophysics*, 599(5-4), pp.121–138. Available at: http://www.scopus.com/inward/ record.url?eid=2-s2.0-0024251901&partnerID=tZOtx3y1 [Accessed June 11, 2015].

Ramos, V. a., Cegarra, M. & Cristallini, E., 1996. Cenozoic tectonics of the High Andes of west-central Argentina (30–36°S latitude). *Tectonophysics*, 259(1-3), pp.185–200. Available at: http://linkinghub.elsevier.com/retrieve/pii/004019519500064X.

Ramos, V. a. & Folguera, a., 2009. Andean flat-slab subduction through time. *Geological Society, London, Special Publications*, 76[1] (5), pp.75–54. Available at: http://sp.lyellcollection.org/cgi/doi/10.1144/SP327.3 [Accessed October 22, 2014].

Ramos, V.A., Cristallini, E.O. & Pe, D.J., 2002. The Pampean ¯ at-slab of the Central Andes. , 15, pp.6–8.

Roeder, D., 1988. Andean-age structure of Eastern Cordillera (Province of La Paz, Bolivia). , 7 (1), pp.23–39.

Roeder, D. & Chamberlain, R., 1995. Structural geology of sub-Andean fold and thrust belt in northwestern Bolivia. Available at: http://archives.datapages.com/data/specpubs/memoir62/23roeder/0459.htm [Accessed June 18, 2015].

Rojas Vera, E. a. et al., 2014. Structure and development of the Andean system between 36° and 39°S. *Journal of Geodynamics*, 73, pp.34–52. Available at: http://linkinghub.elsevier.com/retrieve/pii/S0264370713001336 [Accessed November 27, 2014].

Roperch, P. et al., 2006. Counterclockwise rotation of late Eocene-Oligocene fore-arc deposits in southern Peru and its significance for oroclinal bending in the central Andes. *Tectonics*, 25 (3), p.n/a–n/a. Available at: http://doi.wiley.com/10.1029/2005TC001882 [Accessed October 22, 2014].

Scheuber, E. & Bogdanic, T., 1994. Tectonic development of the north Chilean Andes in relation to plate convergence and magmatism since the Jurassic. *Tectonics of the southern …*. Available at: http://link.springer.com/chapter/10.1007/978-3-642-77353-2_9 [Accessed June 18, 2015].

Sébrier, M. et al., 1988. Tectonics and uplift in Central Andes (Peru, Bolivia and northern Chile) from Eocene to present. *Géodynamique*. Available at: http://www.documentation.ird.fr/hor/fdi:26021 [Accessed June 18, 2015].

Skinner, S.M. & Clayton, R.W., 2013. The lack of correlation between flat slabs and bathymetric impactors in South America. *Earth and Planetary Science Letters*, 371-372, pp.1–5. Available at: http://dx.doi.org/10.1016/j.epsl.2013.04.013.

Stern, C.R., 1991. Role of subduction erosion in the generation of Andean magmas. *Geology*, 19 (1), p.78. Available at: http://www.scopus.com/inward/record.url?eid=2-s2.0-84879879997&partnerID=tZOtx3y1 [Accessed June 18, 2015].

Torres-Carbonell, P.J., Olivero, E.B. & Dimieri, L. V., 2008. Control en la magnitud de desplazamiento de rumbo del Sistema Transformante Fagnano, Tierra del Fuego, Argentina. *Revista Geologica de Chile*, 35(1), pp.63–77. Available at: http://www.scopus.com/inward/record.url?eid=2-s2.0-44149115004&partnerID=tZOtx3y1.

Uba, C.E. et al., 2009. Unsteady evolution of the Bolivian Subandean thrust belt: The role of enhanced erosion and clastic wedge progradation. *Earth and Planetary Science Letters*, 281(3-4), pp.134–146. Available at: http://linkinghub.elsevier.com/retrieve/pii/S0012821X09000983 [Accessed October 25, 2014].